

LayerMix: Enhanced Data Augmentation through Fractal Integration for Robust Deep Learning

Hafiz Mughees Ahmad[†] Dario Morle[‡] Afshin Rahimi[†]
[†]University of Windsor, Canada and [‡]IFIVEO CANADA INC.
 {ahmad54, arahimi}@uwindsor.ca dario@ifiveo.com

Abstract

Deep learning models have demonstrated remarkable performance across various computer vision tasks, yet their vulnerability to distribution shifts remains a critical challenge. Despite sophisticated neural network architectures, existing models often struggle to maintain consistent performance when confronted with **Out-of-Distribution (OOD)** samples, including natural corruptions, adversarial perturbations, and anomalous patterns. We introduce LayerMix, an innovative data augmentation approach that systematically enhances model robustness through structured fractal-based image synthesis. By meticulously integrating structural complexity into training datasets, our method generates semantically consistent synthetic samples that significantly improve neural network generalization capabilities. Unlike traditional augmentation techniques that rely on random transformations, LayerMix employs a structured mixing pipeline that preserves original image semantics while introducing controlled variability. Extensive experiments across multiple benchmark datasets, including CIFAR-10, CIFAR-100, ImageNet-200, and ImageNet-1K demonstrate LayerMix's superior performance in classification accuracy and substantially enhances critical **Machine Learning (ML)** safety metrics, including resilience to natural image corruptions, robustness against adversarial attacks, improved model calibration and enhanced prediction consistency. LayerMix represents a significant advancement toward developing more reliable and adaptable artificial intelligence systems by addressing the fundamental challenges of deep learning generalization. The code is available at <https://github.com/ahmadmughees/layermix>.

Index Terms

Classification, Data Augmentation, Fractals, Robustness, Corruption, Adversarial Attack.

1 INTRODUCTION

Deep Learning (DL) based models have proven highly effective [1]–[3] in training **Computer Vision (CV)** tasks [4]–[11], including but not limited to image classification [12]–[15], object detection [16]–[18], and semantic segmentation [19]–[21]. While these models perform exceptionally well under ideal conditions where the training and test data follow the same distribution, their robustness is often challenged when faced with **Out-of-Distribution (OOD)** samples [22]–[25]. Common **OOD** scenarios include natural corruptions [26], adversarial perturbations [27], and anomaly patterns [28], highlighting the critical need for models to maintain accuracy across distribution shifts. To address this, **Data Augmentation (DA)** has emerged as a widely adopted strategy, where various transformations are applied to existing images to generate synthetic yet diverse training examples [29]–[31]. By expanding the diversity of the training dataset, **DA** can significantly improve the model's robustness against unseen data distribution shifts [32].

DA techniques are traditionally categorized into two main types [33], [34]: 1) Individual augmentations that operate independently on a single data sample to generate new variations. These include both, spatial and affine transformations [2], [35], [36]. 2) Multiple augmentations use multiple samples to synthesize a new sample. It can use the samples from the same dataset or some other data source [37]–[39]. Recently, a new line of research to create complex images has been proposed [40]–[43] where training images are mixed with Structurally Complex Objects, which is often described in terms of the degree of organization [44]. Fractals serve as a classic instance of structurally intricate objects, which were also utilized in the pretraining of image classifiers. [45], [46]. Fractals are label-preserving approach instead of MixUp [37] based approaches where new labels are assigned to synthesized samples, which often results in manifold intrusion [47], [48].

Hendrycks *et al.* [40] created the labels-preserved complex images using the conic combination of fractals and training images. Huang *et al.* [41] used the multi-level mixing approach of pixel, patch, and image for mixing fractals into training samples to generate unique samples. Both of these approaches resulted in improved training accuracy as well as **ML** robustness metrics evaluated on benchmark datasets [25], [49]. These preliminary studies examined the integration of fractals with randomly sampled data in a pipeline characterized by a vast search space, necessitating the use of supplementary training methodologies to enhance optimization. To address this and reduce the dependence on additional training tricks, we have proposed a LayerMix, a structured mixing pipeline that combines unique samples to train a **ML** model, achieving improvements across all benchmark metrics.

The primary contributions of this study are summarized as follows:

- 1) A comprehensive theoretical framework for investigating optimal strategies for mixing fractals.
- 2) A novel mathematically evaluated mixing pipeline, with each step rigorously analyzed.
- 3) Extensive experimental evaluations demonstrating state-of-the-art performance on the CIFAR-10, CIFAR-100, ImageNet-200, and ImageNet benchmarks, achieving substantial improvements in generalization and adversarial robustness compared to existing methods.
- 4) The full open-sourcing of the framework, enabling evaluation of classification models across all metrics in a unified platform, alongside the release of training runs and experimental meta-data on GitHub.

The remainder of this paper is structured as follows: background and literature review are provided in Section 2. Technical details are provided in Section 3 and discussions on the results of the experiments are provided in Section 4. Finally, Section 5 offers concluding remarks and future directions.

2 RELATED WORK

“Data Augmentation methodology can outperform models trained with 1000x more data - Hendryks *et al.* [50]”.

Data augmentation serves as a pivotal technique in deep learning, aiming to enhance the diversity of training datasets by systematically transforming existing data samples. By creating novel and varied instances, these transformations facilitate better regularization and improve the generalization capacity of models. Since the early days of DL, including Convolutional Neural Network (CNN)-based architectures such as LeNet [51], AlexNet [52], and ResNet [12], data augmentation has been a cornerstone in achieving robust performance. It’s significance continues with more recent architectures [53] such as Vision Transformers [54], [55] and Diffusion Networks [56], [57].

Typically, modern DL models have a representation capacity beyond the datasets they are trained on [58]. However, recent research has shown that there are limits past which sample diversity hinders performance. For example, [47] identifies manifold intrusion as a limit where extreme augmentation can cause synthetic labels to collide with labels from the original dataset. To understand these limitations, we standardize the definitions and represent the pipelines in the literature mathematically as a function of data distributions.

2.1 Affinity and Diversity

Modern data augmentation pipelines aggressively increase diversity, even sampling out of distribution data. To understand these pipelines, Lopes *et al.* [59] and Yang *et al.* [60] identify two inversely proportional metrics for analysis. In [59], **affinity** is defined as the difference in model accuracy between the test-set and the augmented test-set, and final training loss value is used to define **diversity**. In [60], **similarity** is defined as Wasserstein distances in the feature space of a trained model, and an aggregation of the eigenvalues of per-class feature embeddings is used to define a **diversity**.

To combine both intuitively for the rest of the article, here we define **affinity** as a measure for the amount that an augmentation pipeline induces label confusion in the model and **diversity** provides a measure for the extent to which the augmentation pipeline extends samples beyond the data manifold. These metrics will naturally be inversely proportional, requiring augmentation algorithms to optimize both to achieve increased model performance jointly.

2.2 Augmentation Pipelines

The goal of data augmentation in deep learning is to improve performance by showing models a more diverse set of inputs than would be feasible using raw data directly. To construct a typical augmentation pipeline, a set of stochastic label-preserving transformations are applied sequentially. We can represent one of these transforms f_k as a sample \mathbf{Y} drawn from a distribution over the output space, conditioned on the input to the transformation \mathbf{z} , i.e., $\mathbf{Y} \sim f_k(\mathbf{y}|\mathbf{z} = \mathbf{Z})$, where k enumerates the different transformations (such as rotation, color jitter, translation). AutoAugment [36] sought to determine a dataset-specific ordering of transformations through reinforcement learning. RandAugment [2] eliminated the need for an order selection by randomly choosing a transformation f_k for each stage in the pipeline. Mathematically, this was equivalent to sampling from $\mathbb{E}_k [f_k(\mathbf{y}|\mathbf{z})]$ rather than a particular $f_k(\mathbf{y}|\mathbf{z})$. This was found to increase sample diversity, ultimately leading to improved performance over AutoAugment. Additionally, RandAugment provided a simpler implementation since each stage in the pipeline is now programmatically identical. One implication of this structure is that the joint distribution over the input-output spaces $\mathbf{x} = [\mathbf{y}^T, \mathbf{z}^T]^T$ of the augmentation stage $p(\mathbf{x}) = p(\mathbf{y}, \mathbf{z}) = p(\mathbf{y}|\mathbf{z})p(\mathbf{z}) = p(\mathbf{z}) \mathbb{E}_k [f_k(\mathbf{y}|\mathbf{z})]$ was **Independant and Identically Distributed (IID)** across all stages in the pipeline.

Outside of augmentation pipeline improvements, additional methods for increasing the efficacy of augmentation were proposed as well. MixUp [37] generated augmented samples by linearly interpolating between two randomly selected images and their corresponding labels, encouraging smoother decision boundaries for classification tasks. Manifold-MixUp [61] performs similar interpolations within the hidden layers of a NN, leading to improved accuracy by enforcing smooth transitions between feature representations. Both of these methods utilized **Vicinal Risk Minimization (VRM)** [62] to increase the diversity of samples.

The IID augmentation stages proposed by RandAugment [2] were combined with the blending stages of MixUp [37] in AugMix [63] to further increase diversity, resulting in improved model performance. This improvement was especially

notable on robustness benchmarks. AugMix followed MixUp regarding the implementation of the blending stage. An arithmetic mean of images was used, weighted by a random convex combination over the images. The images used for blending consisted primarily of augmentation stages applied to the original image and blends thereof. AugMix also included a new term in the loss function named [Jensen–Shannon Divergence \(JSD\)](#) consistency to increase model performance. This new term ensured that the learned representations of an augmented image did not diverge significantly from the representation of the original image. This is a form of affinity as defined in section 2.1.

PixMix [40] built on AugMix [63] through the introduction of fractals for blending, pipeline structure improvements, and increasing the resultant diversity from blending stages. In AugMix, each blending stage would use a weighted arithmetic mean of images. PixMix extended this by considering a mixture of blending methods, similar to the extension RandAugment used on AutoAugment. Mathematically, if a blending method is described as sampling an image \mathbf{Y} from a distribution g_k conditioned on two input images \mathbf{Z}_0 and \mathbf{Z}_1 : $\mathbf{Y} \sim g_k(\mathbf{y}|\mathbf{z}_0 = \mathbf{Z}_0, \mathbf{z}_1 = \mathbf{Z}_1)$, then a PixMix blending stage can be described by sampling from the mixture distribution $q(\mathbf{y}|\mathbf{z}_0, \mathbf{z}_1) = \mathbb{E}_k[g_k(\mathbf{y}|\mathbf{z}_0, \mathbf{z}_1)]$. Specifically, PixMix considered two blending methods: an arithmetic mean and a geometric mean. In addition to the mixture generalization, PixMix diverged from MixUp by considering conic weight combinations to further increase diversity. Although the sum of the weights used in PixMix was not strictly equal to 1, the sampling used ensured that the expected value of the sum would still remain 1. PixMix also introduced fractal images into their augmentation pipeline. Since fractals were unlikely to collide with the data manifold in a label-conflicting manner, they could be used for blending to achieve a large increase in diversity with minimal downsides.

IPMix [41] built on PixMix [40] through considering a variety of pipeline structures, and increasing the diversity of blending stages further by considering more blending methods. In addition to the arithmetic and geometric means considered by PixMix, IPMix also used pixel level and joint pixel-channel (element) mixing. With these adjustments, IPMix enhanced sample diversity and improved model performance. These performance increases were particularly notable on robustness benchmarks.

2.3 Robust Deep Learning

Ensuring the safety of DL systems is a critical aspect of deploying models in real-world applications, particularly in high-stakes environments. The risks associated with unsafe ML deployment, as highlighted in prior research [64]–[66], include severe economic, societal, and ethical consequences. With the advent of Self-Driving Cars [67], [68] and [Large Multimodal Model \(LMM\)](#) [69]–[72], safety concerns have taken center stage, as these models, despite their impressive capabilities are prone to errors and can confidently provide incorrect predictions or fail under adversarial questioning. To address such challenges, various safety measures have been proposed, encompassing robustness, calibration, and anomaly detection, among others. Building on Hendricks *et al.* [40], we categorize safety metrics tasks into four key subdomains, discussed below.

Robustness. Robustness in ML systems pertains to their ability to maintain performance under distributional shifts or adverse conditions. Corruption robustness, for instance, evaluates resistance to natural perturbations encountered in real-world settings. ImageNet-C [25] benchmark, a variant of ImageNet, introduces 15 common corruptions across five levels of severity, serving as a benchmark for assessing models’ robustness under challenging, real-world conditions [50]. It is commonly used as a difficult, held-out test set for models trained on the ImageNet dataset [73]. Further extending the robustness benchmarks, Mintun *et al.* proposed ImageNet-C̄ [26], a complementary set of corruptions for evaluation. ImageNet-R benchmark [50] evaluates abstract visual generalization capability beyond natural corruptions to test model performance against diverse object renditions, such as paintings, cartoons, graffiti, embroidery, origami, sculptures, and toys, reflecting broader variations encountered in real-world scenarios. The dataset contains 200 categories instead of the original 1000 total categories in the ImageNet dataset. Hendrycks *et al.* also introduced ImageNet-P [25], which measures prediction consistency under non-adversarial input perturbations on 10 different perturbation types.

Adversarial robustness. It addresses the challenge of imperceptible image perturbations crafted to mislead models [74]. Studies have noted a trade-off between robustness to adversarial perturbations and accuracy on clean data [75], [76]. In the domain adaptation context, Bashkurova *et al.* [77] explored robustness during test-time adaptation and anomaly detection [78]. Additionally, Yin *et al.* [79] observed that adversarial training, while improving performance under adversarial settings, can degrade robustness against certain corruptions. They suggest that this vulnerability is partly due to the model’s reliance on spurious correlations [80], [81]. Geirhos *et al.* [82] highlight the texture bias present in CNN and demonstrate that training with a diverse set of stylized images can enhance robustness against these shifts. Ensuring robustness in ML models involves making them resilient to various forms of data shifts that may occur during testing.

Calibration. Calibration refers to the alignment between a model’s predicted confidence and its actual accuracy. Properly calibrated predictions are vital in real-world applications where overconfidence can lead to critical errors. Bayesian approaches [83] are widely employed for estimating uncertainty and improving calibration. Recalibration methods, such as those proposed by Kuleshov *et al.* [84], address the miscalibration of credible intervals to ensure reliability. Ovadia *et al.* [85] provide a comprehensive evaluation framework for assessing models’ calibration and accuracy under distributional shifts, highlighting the importance of confidence estimation in dynamic environments.

These advancements highlight the versatility and importance of data augmentation across a wide range of deep learning applications, underscoring its central role in enhancing model performance, particularly in challenging scenarios involving

data corruption or domain shifts. By addressing robustness and calibration aspects, ML safety frameworks are better equipped to mitigate risks, ensuring the deployment of reliable and trustworthy models in real-world scenarios.

3 METHODOLOGY

We introduce LayerMix, a layering-based data augmentation framework designed to balance affinity and diversity and increase both clean accuracy and safety metrics. In our design, we find several areas in previous work where diversity can be eliminated without significantly impacting model performance and reallocate this in new ways to achieve better results. In particular, we introduce covariance between augmentation stages in our pipeline, we employ augmentations on fractals for mixing, we redesign the augmentation pipeline, and reweigh the blending methods used across PixMix [40] and IPMix [41].

3.1 Pipeline Covariance

We determined a simple method for introducing covariance into the augmentation pipeline. We start by sampling a single transformation f_k from a set of possible transformations. Next, we apply the selected transformation f_k for each augmentation stage in our pipeline. Mathematically, this is equivalent to first sampling k from a multinomial distribution, then sampling $\mathbf{Y} \sim f_k(\mathbf{y}|\mathbf{z})$ to apply each augmentation stage in the pipeline. To analyze the covariance between stages, we construct the joint distribution over all stages' input-output spaces \mathbf{x}_n , where n is the index of the stage in the pipeline. Unlike the IID approach described in Section 2.2, stages are only independent after conditioning on the outcome k of the multinomial distribution, allowing for the direct construction of the conditional distribution $p_{\text{layermix}}(\mathbf{x}|k) = \prod_n f_k(\mathbf{x}_n)$. Taking the expected value over k yields the marginal distribution over \mathbf{x} :

$$p_{\text{layermix}}(\mathbf{x}) = \mathbb{E}_k \left[\prod_n f_k(\mathbf{x}_n) \right] \quad (1)$$

Equation (1) is notably different from the corresponding marginal distribution in IID pipelines. Since each stage is marginally independent $p_{iid}(\mathbf{x}_n, \mathbf{x}_m) = p_{iid}(\mathbf{x}_n)p_{iid}(\mathbf{x}_m) \forall n \neq m$, the joint distribution p_{iid} can be expressed as the product over the per-stage mixture distributions:

$$p_{iid}(\mathbf{x}) = \prod_n \mathbb{E}_k [f_k(\mathbf{x}_n)] \quad (2)$$

Using Eq. (1), the auto-covariance matrix over \mathbf{x} can be calculated analytically. Throughout this calculation we consider $x_n \in \mathbb{R}$, the general case follows. To perform this calculation, we first consider the diagonal entries, $\mathbf{K}_{\mathbf{x}_i, \mathbf{x}_i}$, where $p(\mathbf{x}) = p_{\text{layermix}}(\mathbf{x})$ for brevity:

$$\begin{aligned} \mathbf{K}_{\mathbf{x}_i, \mathbf{x}_i} &= \mathbb{E} [X_i^2] - \mathbb{E} [X_i]^2 \\ &= \langle x_i^2, p(x_i) \rangle - \langle x_i, p(x_i) \rangle^2 \\ &= \mathbb{E}_k [\langle x_i^2, f_k(x_i) \rangle] - \mathbb{E}_k [\langle x_i, f_k(x_i) \rangle]^2 \\ &= \mathbb{E}_k [\mu_{ki}^2 + \sigma_{ki}^2] - \mathbb{E}_k [\mu_{ki}]^2 \end{aligned} \quad (3)$$

As a second case, we calculate the off-diagonal entries, $\mathbf{K}_{\mathbf{x}_i, \mathbf{x}_j \neq i}$, where $p(\mathbf{x}) = p_{\text{layermix}}(\mathbf{x})$ for brevity:

$$\begin{aligned} \mathbf{K}_{\mathbf{x}_i, \mathbf{x}_j \neq i} &= \mathbb{E} [X_i X_j] - \mathbb{E} [X_i] \mathbb{E} [X_j] \\ &= \langle x_i x_j, p(x_i, x_j) \rangle - \langle x_i, p(x_i) \rangle \langle x_j, p(x_j) \rangle \\ &= \mathbb{E}_k [\langle x_i x_j, f_k(x_i) f_k(x_j) \rangle] - \mathbb{E}_k [\langle x_i, f_k(x_i) \rangle] \mathbb{E}_k [\langle x_j, f_k(x_j) \rangle] \\ &= \mathbb{E}_k [\langle x_i, f_k(x_i) \rangle \langle x_j, f_k(x_j) \rangle] - \mathbb{E}_k [\langle x_i, f_k(x_i) \rangle] \mathbb{E}_k [\langle x_j, f_k(x_j) \rangle] \\ &= \mathbb{E}_k [\mu_{ki} \mu_{kj}] - \mathbb{E}_k [\mu_{ki}] \mathbb{E}_k [\mu_{kj}] \end{aligned} \quad (4)$$

Using Eq. (3) for the diagonal elements of $\mathbf{K}_{\mathbf{x}_i, \mathbf{x}_j}$ and Eq. (4) for the off-diagonal elements results in the following complete auto-covariance matrix expression:

$$\mathbf{K}_{\mathbf{x}_i, \mathbf{x}_j} = \begin{cases} \mathbb{E}_k [\sigma_{ki}^2] + \mathbb{E}_k [\mu_{ki}^2] - \mathbb{E}_k [\mu_{ki}]^2 & \text{if } i = j \\ \mathbb{E}_k [\mu_{ki} \mu_{kj}] - \mathbb{E}_k [\mu_{ki}] \mathbb{E}_k [\mu_{kj}] & \text{else} \end{cases} \quad (5)$$

The result of this calculation is a relation between the covariance of any two joint input-output image spaces $\text{Cov}(X_i, X_j)$ and low-order statistics of the transformations f_k . This covariance structure can be directly contrasted against the implied covariance structure from the IID pipelines defined by Eq. (2): $\mathbf{K}_{\mathbf{x}_i, \mathbf{x}_j} = \text{diag}(\mathbb{E}_k[\sigma_k^2])$. This approach decreases sample diversity without hindering performance. In combination with this, we increase the magnitude of the transformations f_k to achieve an overall increase in model performance.

3.2 Fractals Augmentation

Fractals can be created through various methods, with iterated function systems being one of the most widely used techniques [86]. However, it demands a significant research and development effort. PixMix [40] simplified it by collecting a total of 14,230 colored fractals from curated repositories on DeviantArt¹ instead of generating a custom set of diverse fractals. They used these fractals to increase the dataset diversity by simply resizing them, followed by a random crop to match the input image size. It was later used by IPMix [41] as well.

Kataoka *et al.* [45] noticed complexity of the fractals provided by shapes and contours is only needed for pertaining a CNN as colors do not provide additional information [86]. To utilize the complexity of the fractals effectively and match with [45], we used a gray-scale version of the 14,230 fractals (collected by PixMix [40]) for blending. We enhanced the diversity of fractals by randomly flipping them horizontally and vertically during training. Additionally, we observed that utilizing gray-scale fractals with earlier methods led to a marked improvement in results (details are provided in Section 4.2.2). Figure 5 shows samples of gray-scale fractals.

3.3 Reweighted Blending

As mentioned in Section 2.2, the blending stage of an augmentation pipeline can be mathematically expressed as sampling from a mixture distribution q over blending methods $g_k: q(\mathbf{y}|\mathbf{z}_0, \mathbf{z}_1) = \mathbb{E}_k [g_k(\mathbf{y}|\mathbf{z}_0, \mathbf{z}_1)]$, where k indexes the blending method. The distribution of blending methods is not specified analytically but rather implied from the definition of the random variable \mathbf{Y} in terms of the input images \mathbf{Z}_0 and \mathbf{Z}_1 , along with other random variables sampled from known distributions. These expressions are shown in Table 1.

TABLE 1: Blending expressions. \odot represents the Hadamard product

Blending Method	Expression	Probability
Arithmetic Mean	$\mathbf{Y} = a\mathbf{Z}_0 + b\mathbf{Z}_1$	33.3%
Geometric Mean	$\mathbf{Y} = 2^{a+b-1} \cdot \mathbf{Z}_0^a \mathbf{Z}_1^b$	33.3%
Pixel Mixing	$\mathbf{Y} = M \odot \mathbf{Z}_0 + (1 - M) \odot \mathbf{Z}_1$	16.6%
Element Mixing	$\mathbf{Y} = M \odot \mathbf{Z}_0 + (1 - M) \odot \mathbf{Z}_1$	16.6%

For the arithmetic and geometric mean expressions (shown in Table 1), both a and b are random variables. In both expressions, $a \sim \frac{1}{2}\mathbf{B}(x|\beta, 1) + \frac{1}{2}\mathbf{B}(x-1|1, \beta)$, and $b \sim \frac{1}{2}\mathbf{B}(x|1, \beta) + \frac{1}{2}\mathbf{B}(-x|1, \beta)$, where \mathbf{B} represents the Beta-Distribution. This sampling results in the conic combination proposed by PixMix [40] and provides a parameter β , the blending ratio, which can be tuned to adjust these blending methods. In the case of pixel and element mixing, M is a boolean mask that determines whether a pixel value is taken from \mathbf{Z}_0 or \mathbf{Z}_1 as defined by IPMix [41].

Through extensive ablation studies, we observed that the arithmetic and geometric blending methods are particularly effective in enhancing clean accuracy by promoting the learning of diverse and discriminative features. Conversely, pixel-wise mixing significantly improves robustness to corruption, likely due to its localized blending effect. To balance these strengths, we adjust the multinomial weights used to construct the mixture distribution q , favoring the arithmetic and geometric methods over the pixel and element methods. In practice, we selected a blending method using the associated probabilities shown in Table 1. This weighting ensured a favorable bias towards methods that contributed to clean accuracy while retaining the robustness benefits of pixel-wise mixing.

3.4 Augmentation Pipeline

The LayerMix pipeline uses a combination of correlated augmentation stages and blending stages. A diagram of the pipeline is shown in Fig. 1, and the pseudo-code is shown in Code Block 1. The final sample produced by LayerMix is selected uniformly between samples 1, 2, and 3 in Fig. 1. We use samples from each of these layers in our pipeline to enable control over the distribution of the diversity of samples produced by our pipeline. Intuitively, sample 1 will have less diversity than sample 2, which in turn will have less diversity than sample 3. By randomly selecting between each of these samples, we are able to reduce the average deviation from the data manifold while still producing highly diverse samples.

1. <https://www.deviantart.com/>

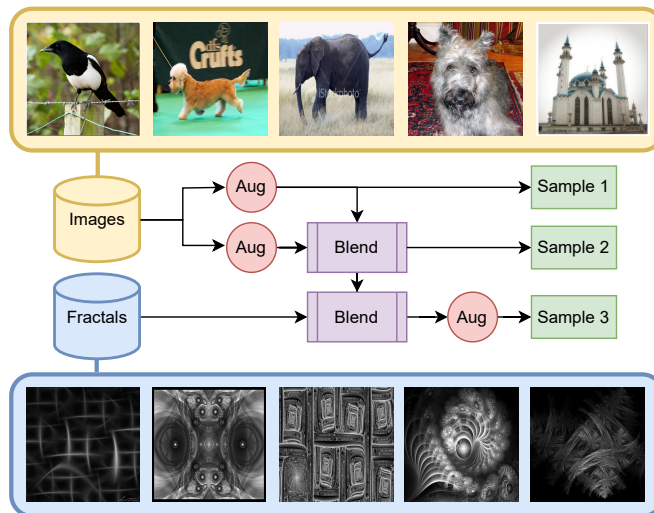


Fig. 1: Complete Pipeline of LayerMix. The resulting image produced by the LayerMix pipeline is uniformly selected from samples 1, 2, and 3 produced by the pipeline. All **Aug** blocks are correlated by the covariance structure described in Section 3.1. All **Blend** blocks are independent and sample from the re-weighted blending mixture distribution described in Section 3.3.

Code Block 1: LayerMix Pipeline.

```

1 def layermix(img, mixing_pic) -> Tensor:
2     step = random.randint(3)
3     img_copy = img.clone()
4     aug_fn = random.choice(aug_fns)
5     img = aug_fn(img, magnitude)
6     if step == 0: return img
7
8     img_2 = aug_fn(img_copy, magnitude)
9     blending = random.choice(blending_fns)
10    img = torch.clip(blending(img, img_2, blending_ratio), 0, 1)
11    if step == 1: return img
12
13    blending = random.choice(blending_fns)
14    img = torch.clip(blending(img, mixing_pic, blending_ratio), 0, 1)
15    return aug_fn(img, magnitude)

```

The fractals in Fig. 1 are sampled uniformly and augmented using the strategy defined in Section 3.2. Through a combination of the intrinsic diversity present in fractals alongside the augmentations, the third sample in the LayerMix pipeline will produce notably more diverse samples than the first two. We find that this combination works well during training as sample 3 is able to effectively blend out the edges of the data manifold over which the model is learning. To enable further control over the diversity of the samples produced by the LayerMix pipeline, we follow [2] and parameterize most of our transformations f_k by an augmentation magnitude parameter m . The transformations are tuned such that any value of m results in a similar increase in sample diversity across all transformations f_k . This tuning was performed by [2] and results in the per-transform value ranges shown in Table 2.

TABLE 2: List of transformations f_k . Transformations with range constrained by the augmentation magnitude m . We build upon torchvision.transforms.v2² library for our experiments.

Operation	Range	Operation	Range	Operation	Range
equalize	-	brightness	0.1 → 1.9	shear_x	-0.3 → +0.3
grayscale	-	posterize	0 → 4	shear_y	-0.3 → +0.3
auto contrast	-	solarize	0 → 1	translate_x	0 → 0.33 (of image size)
		rotate	-30° → +30°	translate_y	0 → 0.33 (of image size)

In the construction of our pipeline, we specifically avoided applying two augmentation stages sequentially. This is due to a form of linearity that emerges from the covariance structure (Section 3.1) when combined with the implementation of the transformations f_k . Mathematically, for many values k , $f_k(\mathbf{y}|\mathbf{z} = \mathbf{Z} \sim f_k(\mathbf{y}|\mathbf{z}; am); bm) \approx f_k(\mathbf{y}|\mathbf{z}; (a + b)m)$. Intuitively, if f_k represents a rotation by $a \sim \mathcal{N}(0, m)$ degrees, then the result of applying f_k twice would be a rotation by $a \sim \mathcal{N}(0, 2m)$ degrees. While this is not a precise description since not all transformations have parameters that can be linearly combined and parameters are not always sampled according to a normal distribution, it can be extended to show the approximate linearity for most of the transformations described in Table 2. Hence, we utilize blending stages as a form of non-linearity to avoid augmentation stages from collapsing in our pipeline.

We have extended these ideas by exploring new strategies for label-preserving augmentations, further improving model generalization and corruption resistance. Our proposed approach draws inspiration from PixMix [40] and IPMix [41] but introduces novel techniques to leverage layered and effective information fusion strategies. By integrating diverse patterns from multiple layers, our method enables the training of models that are more robust to data corruption and domain shifts, pushing the boundaries of existing augmentation techniques.

4 EXPERIMENTS

To assess the performance of our proposed method LayerMix, we have used a similar experimentation setting as PixMix [40] on benchmark datasets i.e., CIFAR-10, CIFAR-100 [87], and ImageNet-1K [88] for training and evaluation of the models on classification accuracy. We have also done rigorous experiments on ImageNet-200 [50] dataset. We also evaluated the robustness of performance across various safety-related tasks on corrupted versions of the test sets. For a fair comparison to earlier methods, any difference to the experimentation setting of PixMix is especially highlighted. IPMix [41] uses JSD Loss proposed by Augmix [63] instead of standard Binary Cross Entropy (BCE) Loss [89]. It uses 3 times the memory but provides better convergence. Therefore, we trained IPMix without JSD Loss for a fair comparison. We have highlighted the performance improvement with JSD loss for LayerMix as well.

We benchmark our approach against state-of-the-art data augmentation techniques, such as MixUp [37], CutMix [90], AugMix [63], RandomErase [3] and recent methods, including PixMix [40] and IPMix [41]. Standard augmentations such as random cropping and flipping serve as baseline. These methods vary in complexity, with strategies ranging from pixel-wise interpolations (MixUp) to advanced augmentation pipelines (AugMix, IPMix). PixMix leverages neural style transfer and augmentation sampling to enhance robustness, requiring fewer augmentations per image than AugMix. IPMix introduces a hierarchical blending strategy inspired by iterative and progressive mixing, offering improvements in both clean accuracy and robustness metrics.

4.1 Evaluation Benchmarks and Metrics

We evaluate our methodology using the benchmark datasets CIFAR-10, CIFAR-100 [87], ImageNet-200 [50], and ImageNet-1K [88] dataset, alongside their respective robustness benchmarks across 4 distinct ML safety tasks. All methods are initially trained on the clean versions of CIFAR-10, CIFAR-100, and ImageNet datasets before being tested on the tasks outlined below.

4.1.1 Corruption Robustness:

In this task, the objective is to classify corrupted images from the CIFAR-10-C, CIFAR-100-C, and ImageNet-C datasets (introduced by [25]). To quantify performance, we use the mean corruption error (mCE) metric, which measures the classification error averaged across all 15 (+4 supplementary) corruption types and 5 levels of severity for each type. A lower mCE indicates better robustness to corruption. We also evaluated on the CIFAR-10- \bar{C} , CIFAR-100- \bar{C} , ImageNet-200- \bar{C} , ImageNet-1k- \bar{C} datasets, introduced by [26], that has 10 additional corruptions for robustness evaluation.

Furthermore, supplementary datasets such as ImageNet-R [50] dataset measure robustness to rendition variations such as art, cartoons, graffiti, embroidery, toys, and video game renditions of ImageNet classes. ImageNet-R has renditions of 200 ImageNet classes, resulting in 30,000 images. The datasets span diverse settings, enabling a comprehensive evaluation of clean accuracy, robustness to corruptions, prediction consistency, calibration, and anomaly detection.

4.1.2 Prediction Consistency:

This task aims to ensure the consistent classification of sequences of perturbed images from the CIFAR-100-P and ImageNet-P datasets where each sample is a sequence of images undergoing gradual perturbations such as zoom, translation, or brightness changes. These sequences enable assessing stability in predictions under minor shifts. The primary metric used here is the mean flip probability (mFP) introduced by [25], which represents the likelihood that adjacent frames in a sequence are assigned different predicted classes. Mathematically, this can be expressed as:

$$\text{mFP} = \mathbb{P}_{x \sim S} (f(x_i) \neq f(x_{i-1})), \quad (6)$$

2. <https://pytorch.org/vision/0.20/>

where x_i denotes the i -th image in a temporal sequence. For non-temporal sequences, such as those with progressively increasing noise levels within sequence S , the metric is adapted as:

$$\text{mFP} = \mathbb{P}_{x \sim S} (f(x_i) \neq f(x_1)). \quad (7)$$

In both cases, a lower mFP indicates greater consistency in the model’s predictions. Sometimes it is also aided by the consistency of top-5 predictions under perturbations. We define a distance metric $d(\tau(x), \tau(x'))$ between the permutations $\tau(x)$ and $\tau(x')$ representing the ranked predictions of a model f . This metric penalizes changes in the top-5 predictions as follows:

$$d(\tau(x), \tau(x')) = \sum_{i=1}^5 \sum_{j=\min\{i, \sigma(i)\}+1}^{\max\{i, \sigma(i)\}} \mathbb{1}(1 \leq j - i \leq 5), \quad (8)$$

where $\sigma = (\tau(x))^{-1}\tau(x')$. The mean Top-5 Distance (mT5D) is the average of T5D_p^f values across all perturbation sequences, providing a measure of top-5 consistency under perturbations.

4.1.3 Adversarial Robustness:

In this task, the objective is to classify images that have been adversarially perturbed using the [Projected Gradient Descent \(PGD\)](#) method [91]. Specifically, we consider untargeted attacks on CIFAR-10 and CIFAR-100, with an ℓ_∞ perturbation budget of $2/255$ and 20 optimization steps. The performance metric for this task is the classifier error rate, where a lower error rate indicates better robustness to adversarial perturbations. We do not include results for ImageNet models in our tables, as all tested methods experience a complete drop in accuracy to zero under this attack budget. This was also observed by PixMix [40].

4.1.4 Calibration:

This task evaluates the model’s ability to produce calibrated prediction probabilities that align with the empirical frequency of correctness. For instance, if a model predicts a 70% probability of rain on ten occasions, we expect it to be correct approximately 7 out of those 10 times. Formally, we aim for the model’s posterior probabilities to satisfy:

$$\mathbb{P}\left(Y = \arg \max_i f(X)_i \mid \max_i f(X)_i = C\right) = C \quad (9)$$

where X and Y are random variables representing the data distribution, and $f(X)_i$ denotes the predicted probability for class i . To quantify calibration, we use the root mean square (RMS) calibration error [92], defined as:

$$\text{RMS Calibration Error} = \sqrt{\mathbb{E}_C \left[\left(\mathbb{P}(Y = \hat{Y} \mid C = c) - c \right)^2 \right]} \quad (10)$$

where C represents the model’s confidence that its predicted label \hat{Y} is correct. We employ adaptive binning [93] to compute this metric, with lower values indicating better calibration. We calculate the calibration using all the robustness datasets.

4.2 CIFAR Results

4.2.1 Training Setup.

For the CIFAR experiments, we employ a WideResNet-40-4 (WRN-40-4) architecture [13] with a dropout rate of 0.3. The initial learning rate is set to 0.1 and is adjusted throughout training using a cosine annealing schedule [94] with a weight decay of 0.0005. For the LayerMix experiments, we set the hyperparameters $\text{magnitude} = 8$ and $\text{blending_ratio} = 3$. This setup ensures a fair comparison across the different augmentation strategies. We used $\beta = 3$ and $k = 3$ for all PixMix and IPmix experiments for CIFAR-10/100. All CIFAR experiments were conducted using one RTX3060 [Graphical Processing Unit \(GPU\)](#).

4.2.2 Experiments.

As shown in Table 3, our proposed method, LayerMix, consistently outperforms the standard baseline as well as other state-of-the-art methods across all evaluated safety metrics. LayerMix performs better than all other approaches on tasks such as Corruption, Consistency, and Calibration. Notably, it significantly enhances confidence calibration, achieving exceptionally low calibration errors on CIFAR-100. Regarding corruption robustness, the improvements on CIFAR-100-C and CIFAR-100- \bar{C} are particularly substantial, with the mean corruption error (mCE) reduced by 5.2% and 3.3% respectively relative to PixMix and by 19.7% and 14.1% compared to the baseline. Prediction consistency, measured via mFP, shows that our method achieves the lowest flip rates compared to PixMix and IPmix. Calibration performance is significantly enhanced. Our Method improves Adversarial robustness experiments against baseline but is second best overall against PGD attacks in CIFAR-10. Detailed results on all the metrics on CIFAR-100 are presented in Table 4. We also analyzed individual [Corruption Error \(CE\)](#) values for various methods on CIFAR-100-C in Fig. 2 and noticed LayerMix improves on all the corruption types.

TABLE 3: CIFAR-10 and CIFAR-100 results with WRN-40-4 model for four distinct safety metrics. **Bold** is best, Underline is second best.

		Baseline	Cutout	Mixup	CutMix	Auto Augment	AugMix	PIXMIX	IPMix	LayerMix
CIFAR-10	Corruptions (\downarrow)	26.4	25.9	21.0	26.5	22.2	12.4	12.1	<u>9.5</u>	9.4
	Consistency (\downarrow)	3.4	3.7	2.9	3.5	3.6	<u>1.7</u>	1.9	1.6	1.6
	Adversaries (\downarrow)	91.3	96.0	93.3	92.1	95.1	86.8	83.2	86.8	<u>83.6</u>
	Calibration (\downarrow)	22.7	17.8	12.1	18.6	14.8	9.4	<u>2.4</u>	4.4	2.1
CIFAR-100	Corruptions (\downarrow)	50.0	51.5	48.0	51.5	47.0	35.4	35.5	<u>30.8</u>	30.3
	Consistency (\downarrow)	10.7	11.9	9.5	12.0	11.2	6.5	6.3	<u>6.0</u>	5.6
	Adversaries (\downarrow)	96.8	98.5	97.4	97.0	98.1	95.6	92.4	<u>95.0</u>	95.5
	Calibration (\downarrow)	31.2	31.1	13.0	29.3	24.9	18.8	<u>7.0</u>	10.3	5.9

TABLE 4: Full results for CIFAR-100 with WRN-40-4 model. LayerMix with $m = 8$ and $\beta = 5$ does result in clean error of 2.4 but for standardization across all WRN-40-4 experiments, we report results of $m = 8$ and $\beta = 3$ here. **Bold** is best, Underline is next best.

	Accuracy	Robustness		Consistency		Adversaries	Calibration		
	Clean Error	C mCE	\bar{C} mCE	CIFAR-P mFP	mT5D	PGD Error	Clean RMS	C RMS	\bar{C} RMS
Baseline	21.3	50.0	52.0	10.7	2.7	96.8	14.6	31.2	30.9
Cutout	19.9	51.5	50.2	11.9	2.7	98.5	11.4	31.1	29.4
Mixup	21.1	48.0	49.8	9.5	3.0	97.4	10.5	13.0	12.9
CutMix	<u>20.3</u>	51.5	49.6	12.0	3.0	97.0	12.2	29.3	26.5
AutoAugment	19.6	47.0	46.8	11.2	2.6	98.1	9.9	24.9	22.8
AugMix	20.6	35.4	41.2	6.5	1.9	95.6	12.5	18.8	22.5
OE	21.9	50.3	52.1	11.3	3.0	97.0	12.0	13.8	13.9
PixMix	20.4	35.5	41.2	6.3	<u>1.7</u>	92.4	<u>7.0</u>	<u>10.5</u>	11.3
IPMix	20.4	<u>30.8</u>	<u>39.4</u>	<u>6.0</u>	<u>1.7</u>	<u>95.0</u>	10.3	13.0	17.8
LayerMix	20.7	30.3	37.9	5.6	1.6	95.5	5.9	8.0	<u>11.9</u>

4.2.3 JSD loss and Optimal Hyperparameters.

We also compared our method with the experimentation setting of IPMix, which uses JSD loss instead of BCE loss. We also compared PixMix and IPMix by using grayscale and colored fractals. As mentioned in the Table 5, just by using gray-scale fractals instead of colored fractals with PixMix, we can improve corruption robustness performance; however, it negatively impacts the clean accuracy. Gray-scale fractals improve the IPMix performance on classification, robustness and consistency. We also note that gray-scale fractals slightly hurt adversarial performance in all methods. LayerMix trained with JSD loss can surpass IPMix with 1.12% on clean accuracy and 2.77% on Adversarial Error. Few other methods [31], [39] trained models for 400, 600, or 1,200 epochs due to high regularization provided by augmentation methods, so we also trained LayerMix for 400 epochs and noticed significant performance improvement over all other methods. We also evaluated the robustness of our pipeline hyperparameters in different combinations (as shown in Table 6) and noticed different combinations of magnitude m and blending ratio β result in a slight improvement in metrics. However, the overall metrics remain in the same error margin of the CNN.

4.2.4 Other Models.

We have also trained WideResNet-28-10 (WRN-28-10) [13], ResNet-18 [12] and ResNext-28 [95] models for comparison with different models. As suggested by the original authors of the respective models, WRN models were trained for 100 epochs, while ResNet-18 and ResNeXt-29 were trained for 200 epochs, keeping all other settings the same. Based on Table 7, we note that ResNeXt-29, having 6.9 Million parameters trained on 200 epochs, surpasses the WRN-40-4 model with 8.9 Million parameters trained with 100 epochs, suggesting heavy augmentation pipelines require more epochs to generalize better. Furthermore, WRN-28-10, having more parameters, surpasses the WRN-40-4 model in similar settings. We compare PixMix and IPMix trained with colored fractals. At the same time, we use gray-scale fractals for LayerMix, surpassing all the other methods on robustness and consistency metrics while being comparable in other metrics.

4.3 ImageNet Results

The ImageNet-1K dataset encompasses 1,000 categories derived from WordNet noun synsets, covering a broad range of objects, including fine-grained distinctions. It includes 1.28 million color images, commonly resized to a resolution of 224×224 pixels for our experiments. We use its validation set, containing 50,000 images, to measure clean accuracy.

TABLE 5: Comparison with experimentation settings of JSD loss with grayscale fractals on Cifar-100 dataset with WRN-40 model. We implemented their settings to the best of our knowledge. (●●) represents the original fractals in grayscale while (●●●) represents the grayscale fractals. ⊗ authors proposed settings. **Bold** is best and underline is second best.

Model	JSD	Fractals	Classification Error(↓)	Robustness mCE(↓)	Adversaries Error(↓)	Consistency mFR(↓)
Baseline	×	×	20.99	51.03	97.04	11.02
PixMix⊗	×	●●	20.36	35.54	92.55	6.16
PixMix	×	●●●	20.56	35.01	97.49	6.54
IPMix	×	●●	20.35	30.84	94.92	5.85
IPMix	×	●●●	20.21	30.68	95.96	5.92
LayerMix	×	●●	20.77	31.11	92.66	5.62
LayerMix	×	●●●	20.70	30.34	95.49	5.55
PixMix	✓	●●	18.46	34.04	86.67	5.91
PixMix	✓	●●●	18.63	32.79	94.74	5.98
IPMix⊗	✓	●●	19.33	28.78	91.84	4.66
IPMix	✓	●●●	19.13	28.29	91.93	<u>4.57</u>
LayerMix	✓	●●	18.73	29.82	86.63	<u>5.49</u>
LayerMix	✓	●●●	18.01	28.89	89.07	5.30
LayerMix (400 epochs)	×	●●	19.41	28.48	92.25	5.28
LayerMix (400 epochs)	×	●●●	18.77	<u>27.63</u>	96.14	5.09
LayerMix (400 epochs)	✓	●●	<u>18.36</u>	27.98	<u>81.41</u>	5.32
LayerMix (400 epochs)	✓	●●●	17.79	27.12	84.54	5.18

TABLE 6: Performance metrics for different combinations of corruption magnitude vs blending ratio on Cifar-100 dataset with WRN-40 model.

Magnitude-Blending	Classification Error(↓)	Robustness mCE(↓)	Adversaries Error(↓)	Calibration RMS(↓)	Consistency mFR(↓)
5-3	20.51	30.24	95.29	6.25	5.49
5-4	20.73	30.64	95.24	6.93	5.53
5-5	20.62	31.07	94.37	6.84	5.65
6-3	20.96	30.55	95.49	6.00	5.66
6-4	20.79	30.75	94.66	6.76	5.49
6-5	20.49	30.96	94.88	7.17	5.48
7-3	20.80	30.49	95.67	6.33	5.51
7-4	20.71	30.74	95.25	6.49	5.41
7-5	20.47	30.97	94.81	6.94	5.37
8-3	20.70	30.34	95.49	5.92	5.55
8-4	20.72	30.79	94.92	6.50	5.45
8-5	20.42	30.82	95.15	6.40	5.36
mean (std)	20.66 (±0.15)	30.70 (±0.37)	95.10(±0.37)	6.54 (±0.37)	5.49 (±0.09)

ImageNet-200 uses the same 200 classes as ImageNet-R [50], a subset of 200 classes of ImageNet. It is important to note that ImageNet-200 is not the same as Tiny-ImageNet-200 [96], which uses a different subset of classes.

4.3.1 Training Setup.

For the ImageNet experiments, we trained ResNet-50 architecture [12]. Following PixMix [40], we also fine-tuned the pre-trained model for 90 epochs, as regularization methods require more epochs to converge. The initial learning rate is set to 0.01 and is adjusted throughout training using a cosine annealing schedule [94] with a batch size of 256. For the LayerMix experiments, we set the hyperparameters $magnitude = 8$ and $blending_ratio = 3$. We used $\beta = 4$, $k = 4$, and $magnitude = 1$ for all PixMix and IPmix experiments. All ImageNet experiments were conducted using one RTX TITAN GPU.

TABLE 7: Performance metrics for different model architectures for CIFAR-100.

Model (Params)	Epochs	Type	Classification Error(↓)	Robustness mCE(↓)	Adversaries Error(↓)	Consistency mFR(↓)	Calibration RMS(↓)
WRN-40-4 (8.9M)	100	baseline	20.99	51.03	97.04	11.02	14.24
		PixMix	20.36	35.54	92.41	6.16	7.00
		IPMix	20.35	30.84	94.98	5.85	10.31
		LayerMix	20.70	30.34	95.49	5.55	5.92
WRN-28-10 (36.5M)	100	baseline	19.08	48.39	96.50	9.62	9.79
		PixMix	18.42	32.35	92.60	5.67	7.24
		IPMix	18.81	28.58	94.84	5.32	9.21
		LayerMix	18.05	27.41	95.24	4.94	5.83
ResNet-18 (11.2M)	200	baseline	21.49	50.40	97.06	10.77	6.99
		PixMix	21.25	34.72	95.14	6.76	7.25
		IPMix	22.22	31.66	96.67	6.47	8.37
		LayerMix	21.37	30.69	95.87	5.96	6.95
ResNeXt-29 (6.9M)	200	baseline	19.98	52.06	98.64	12.05	5.50
		PixMix	18.65	34.15	98.57	6.88	6.01
		IPMix	20.39	30.28	98.02	6.22	7.55
		LayerMix	18.94	28.75	98.71	5.78	6.51

CIFAR-100-C: error rate heatmap

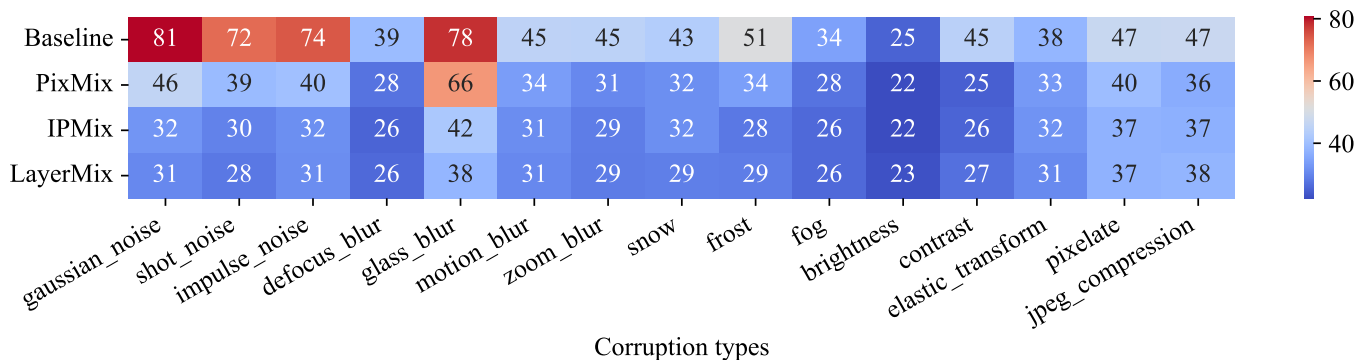


Fig. 2: Corruption Error values for various methods on CIFAR-100-C.

4.3.2 Performance Analysis

Table 8 presents our comprehensive evaluation of ImageNet-200. Our findings demonstrate that LayerMix consistently surpasses conventional augmentation techniques across all safety metrics. This stands in notable contrast to alternative augmentation approaches, which occasionally underperform relative to baseline methods (standard cropping and flipping operations). Significantly, LayerMix represents the first augmentation strategy to achieve comprehensive Pareto improvements over baseline measurements across diverse safety criteria.

In terms of corruption robustness, LayerMix demonstrates exceptional performance, surpassing current state-of-the-art augmentation techniques. Specifically, we observed a 14.26% improvement in mCE compared to the baseline and a 3.54% enhancement over the next best method (PixMix). Regarding rendition robustness on ImageNet-R, LayerMix exhibited superior performance across all methods i.e., 8.13% over baseline and 0.5% over the next best. In contrast, LayerMix achieves a 0.5% improvement in clean accuracy over baseline but has 0.24% less than best(CutMix). LayerMix does outperform CutMix on all other metrics, highlighting its practical advantage for real-world applications where maintaining performance under ideal conditions remains crucial. We also provide the individual corruption improvement on Imagnet-200-C and ImageNet-200-C in the form of heatmaps in Fig. 3 and Fig. 4. On ImageNet-1K, we observe similar trends as mentioned in Table 9.

Overall, the results highlight the efficacy of our approach in enhancing safety measures without compromising clean accuracy. These improvements make it an appealing choice for real-world applications where robustness and reliability are critical.

TABLE 8: Full results for ImageNet-200. **Bold** is best, and underline is second best.

	Accuracy		Robustness				Consistency		Calibration			
	Clean@1	Clean@5	C	\bar{C}	R@1	R@5	ImageNet-P		Clean	C	\bar{C}	R
	Error	Error	mCE	mCE	Error	Error	mFR	mT5D	RMS	RMS	RMS	RMS
Baseline	8.53	1.96	44.03	44.89	65.40	49.41	43.34	6.76	<u>2.60</u>	11.71	15.04	23.16
Cutmix	7.81	1.87	45.26	44.49	66.46	51.05	47.54	7.45	4.88	10.51	12.90	21.45
Mixup	<u>7.87</u>	1.72	37.60	37.47	62.24	46.31	43.27	6.80	3.96	7.08	11.07	<u>16.23</u>
RE	8.21	1.65	44.01	44.48	66.19	50.40	45.12	7.00	3.38	12.39	14.88	24.26
AugMix	8.09	1.75	35.40	38.61	58.94	43.25	43.91	6.81	2.75	6.97	12.29	18.79
PixMix	7.97	1.86	<u>33.31</u>	27.57	<u>57.64</u>	<u>41.96</u>	47.21	7.26	2.94	<u>5.16</u>	5.48	16.11
IPMix	7.93	<u>1.69</u>	34.06	36.03	59.65	43.41	42.54	6.63	2.99	6.63	10.54	19.33
LayerMix	8.05	<u>1.69</u>	29.77	<u>29.26</u>	57.27	41.46	<u>43.09</u>	<u>6.67</u>	2.46	4.72	<u>6.44</u>	16.63

TABLE 9: Comparison on ImageNet-1K. **Bold** is best, and underline is second best.

	Accuracy		Robustness				Calibration			
	Clean@1	Clean@5	C	\bar{C}	R@1	R@5	Clean	C	\bar{C}	R
	Error	Error	mCE	mCE	Error	Error	RMS	RMS	RMS	RMS
baseline	23.84	7.12	60.19	61.29	63.84	47.12	5.60	11.91	20.73	19.71
PixMix	23.73	7.05	52.87	47.82	59.65	44.23	4.43	5.90	6.68	10.20
IPMix	22.51	6.41	53.64	54.28	60.94	45.06	3.66	6.80	11.06	11.20
LayerMix(1m-4 β)	23.53	6.79	53.15	49.38	60.14	44.40	4.06	5.83	8.21	10.38
LayerMix(8m-3 β)	23.57	6.88	51.04	48.05	59.59	43.97	4.76	5.68	7.04	10.42

ImageNet-200-C: Error Rate Heatmap

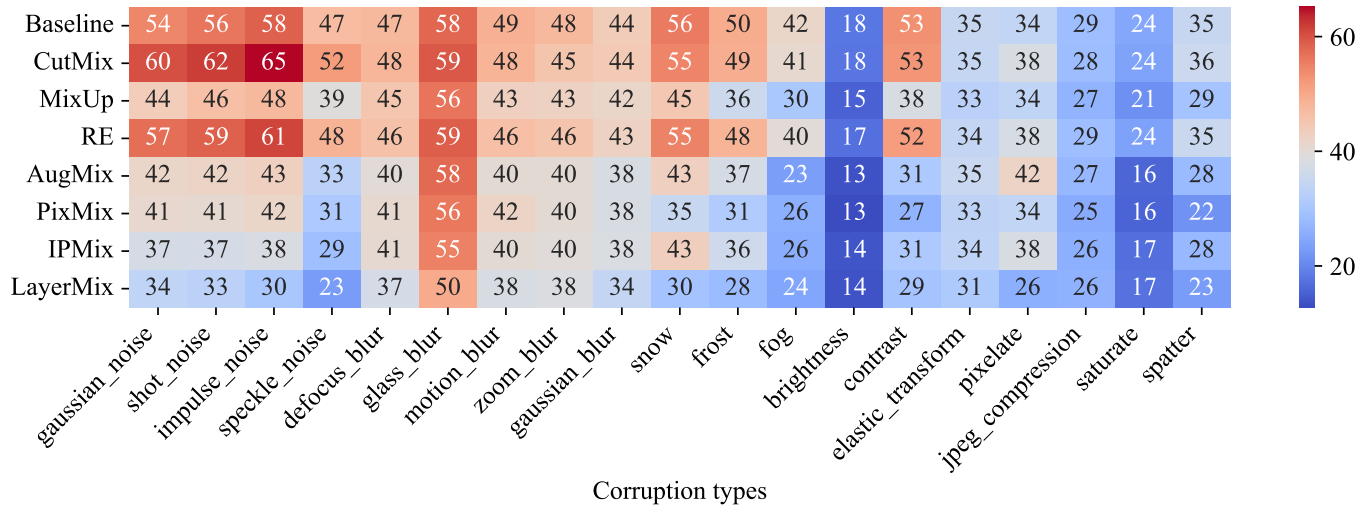
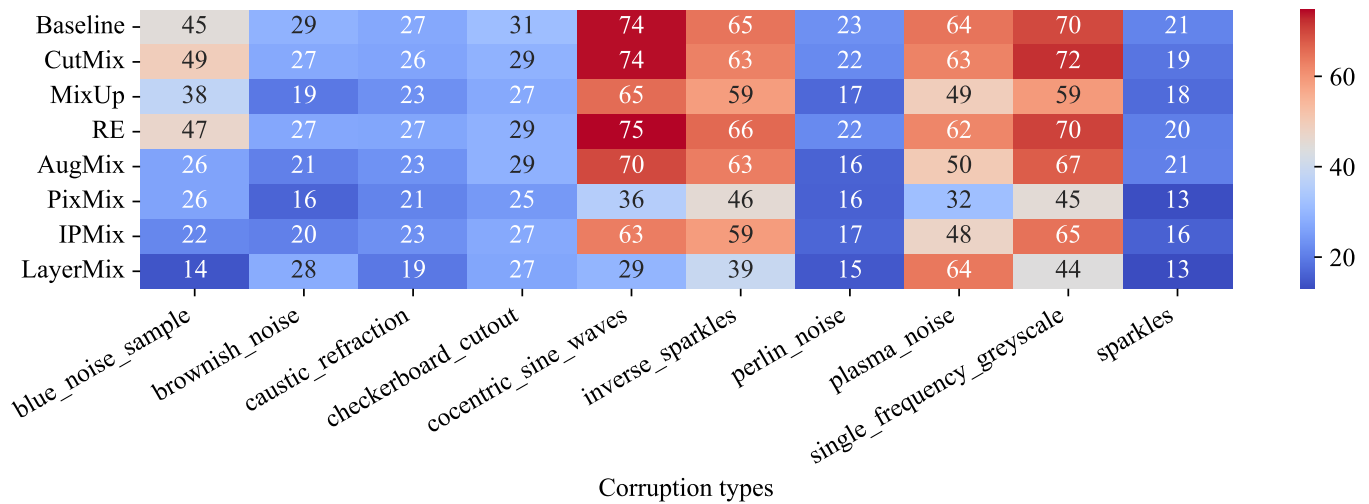


Fig. 3: Individual Corruption Error (CE) values for various methods on ImageNet-200-C

ImageNet-200- \bar{C} : error rate heatmapFig. 4: Corruption Error (CE) values for various methods on CIFAR-100- \bar{C} .

5 CONCLUSION

This research introduces LayerMix, a novel and efficient data augmentation methodology that demonstrates significant advancement in ML safety measures. The distinctive aspect of LayerMix lies in its innovative approach to augmentation complexity, specifically through the strategic integration of fractal patterns and feature visualizations into the training pipeline. LayerMix introduces covariance between augmentation stages of the pipeline. In this work, we consider a particular structure selected due to its ease of implementation and improved results. This represents a departure from conventional augmentation techniques, offering a more sophisticated approach to model training. Our comprehensive evaluation framework encompassed multiple critical dimensions of ML safety, including Corruption robustness, Rendition robustness, Prediction consistency, Adversarial robustness, and Confidence calibration. The empirical results demonstrate LayerMix's exceptional performance across this broad spectrum of safety metrics. These findings suggest promising directions for future research in robust ML systems, particularly in applications where model reliability and safety are paramount. The success of LayerMix in simultaneously addressing multiple safety concerns while maintaining computational efficiency opens new avenues for developing increasingly robust and reliable ML systems.

5.1 Shortcomings and Future Directions

While LayerMix demonstrates significant advancements, several limitations highlight opportunities for future research. One notable shortcoming is the availability of unique fractal patterns that generalize optimally across all datasets or domains. Additionally, the computational overhead introduced by the augmentation process, although efficient compared to similar methods, may still pose challenges to some. The scalability of LayerMix to large-scale datasets and models also warrants further investigation, particularly in scenarios where training efficiency is critical.

Future research could focus on extending the LayerMix framework to adaptively select or generate augmentation patterns during the training process. It could contrast different covariance structures between augmentation stages to determine the effects of our proposed structure. Additionally, it is possible to introduce covariance between blending stages which was not investigated in this work. The utilization of LayerMix in downstream applications, like object detection and segmentation needs to be investigated. Exploring the integration of LayerMix with unsupervised or self-supervised learning paradigms could further enhance its robustness and applicability. Moreover, addressing its computational demands through hardware-aware optimizations or lightweight implementations would improve its usability in real-world applications. Expanding the evaluation framework to include additional safety metrics and diverse benchmarks could provide a more comprehensive understanding of its performance. These directions could collectively contribute to the evolution of robust ML systems that are both scalable and versatile.

SUPPLEMENTARY MATERIALS

All of our code, training runs, and experimental meta-data to reproduce results are available at <https://github.com/ahmadmughees/layermix>.

AUTHORS CONTRIBUTIONS

Hafiz Mughees Ahmad: Conceptualization, Methodology, Software, Investigation, Validation, Data curation, Formal analysis, Visualization, Resources, Writing - Original draft preparation. **Dario Morle:** Investigation, Validation, Formal Analysis, Software, Writing - Original draft preparation, Conceptualization. **Afshin Rahimi:** Funding acquisition, Project administration, Resources, Supervision, Writing - Review & Editing.

FUNDING

This study is supported by IFIVEO CANADA INC., Mitacs through IT16094, and the University of Windsor, Canada.

INSTITUTIONAL REVIEW

Not applicable.

INFORMED CONSENT

Not applicable.

DATA AVAILABILITY

The data used in this study is fully open-source and publicly available and links to each item are mentioned in Table 10.

3. list of classes is available at github.com/ahmadmughees/layermix

TABLE 10: Publically available data sources.

CIFAR-10/100	www.cs.toronto.edu/~kriz/cifar.html
CIFAR-10/100-C	github.com/hendrycks/robustness
CIFAR-10- \bar{C}	github.com/facebookresearch/augmentation-corruption
CIFAR-100- \bar{C}	github.com/ahmadmughees/layermix
CIFAR-10/100-P	github.com/hendrycks/robustness
ImageNet-1K	www.image-net.org
ImageNet-C	github.com/hendrycks/robustness
ImageNet- \bar{C}	github.com/facebookresearch/augmentation-corruption
ImageNet-P	github.com/hendrycks/robustness
ImageNet-R	github.com/hendrycks/imagenet-r
ImageNet-200	ImageNet-1k subset with the same classes as ImageNet-R ³

CONFLICT OF INTEREST

Author Dario Morle was employed by the company IFIVEO CANADA Inc. The authors declare that the research was conducted in the absence of any commercial or financial relationships that could be construed as a potential conflict of interest.

ACKNOWLEDGEMENT

We like to thank Dr. Zaigham Zaheer from MBZUAI for the helpful discussion during this project.

REFERENCES

- [1] E. D. Cubuk, B. Zoph, D. Mane, V. Vasudevan, and Q. V. Le, "Autoaugment: Learning augmentation strategies from data," in *Proceedings of the IEEE/CVF Conference on Computer Vision and Pattern Recognition (CVPR)*, June 2019.
- [2] E. D. Cubuk, B. Zoph, J. Shlens, and Q. V. Le, "RandAugment: Practical automated data augmentation with a reduced search space," in *Proceedings of the IEEE/CVF Conference on Computer Vision and Pattern Recognition (CVPR) Workshops*, June 2020.
- [3] Z. Zhong, L. Zheng, G. Kang, S. Li, and Y. Yang, "Random erasing data augmentation," in *AAAI Conference on Artificial Intelligence*, 2017.
- [4] X. Wang, C. Chen, Y. Cheng, and Z. J. Wang, "Zero-shot image classification based on deep feature extraction," *IEEE Transactions on Cognitive and Developmental Systems*, vol. 10, pp. 432–444, 2018.
- [5] X. Zhai, X. Wang, B. Mustafa, A. Steiner, D. Keysers, A. Kolesnikov, and L. Beyer, "LiT: Zero-shot transfer with locked-image text tuning," *2022 IEEE/CVF Conference on Computer Vision and Pattern Recognition (CVPR)*, pp. 18 102–18 112, 2021.
- [6] X. Gu, T.-Y. Lin, W. Kuo, and Y. Cui, "Open-vocabulary object detection via vision and language knowledge distillation," in *International Conference on Learning Representations*, 2021.
- [7] D. Maturana and S. A. Scherer, "VoxNet: A 3D convolutional neural network for real-time object recognition," *2015 IEEE/RSJ International Conference on Intelligent Robots and Systems (IROS)*, pp. 922–928, 2015.
- [8] B. Yang, W. Luo, and R. Urtasun, "PIXOR: Real-time 3D object detection from point clouds," *2018 IEEE/CVF Conference on Computer Vision and Pattern Recognition*, pp. 7652–7660, 2018.
- [9] J. Mao, Y. Xue, M. Niu, H. Bai, J. Feng, X. Liang, H. Xu, and C. Xu, "Voxel transformer for 3D object detection," *2021 IEEE/CVF International Conference on Computer Vision (ICCV)*, pp. 3144–3153, 2021.
- [10] F. Wang, X. Xiang, J. Cheng, and A. L. Yuille, "NormFace: L2 hypersphere embedding for face verification," *Proceedings of the 25th ACM international conference on Multimedia*, 2017.
- [11] H. Wang, Y. Wang, Z. Zhou, X. Ji, Z. Li, D. Gong, J. Zhou, and W. Liu, "CosFace: Large margin cosine loss for deep face recognition," *2018 IEEE/CVF Conference on Computer Vision and Pattern Recognition*, pp. 5265–5274, 2018.
- [12] K. He, X. Zhang, S. Ren, and J. Sun, "Deep residual learning for image recognition," in *Proceedings of the IEEE Conference on Computer Vision and Pattern Recognition*, 2016, pp. 770–778.
- [13] S. Zagoruyko and N. Komodakis, "Wide Residual Networks," in *British Machine Vision Conference 2016*. York, France: British Machine Vision Association, Jan. 2016. [Online]. Available: <https://enpc.hal.science/hal-01832503>
- [14] C. Szegedy, S. Ioffe, V. Vanhoucke, and A. A. Alemi, "Inception-v4, inception-resnet and the impact of residual connections on learning," in *Thirty-First AAAI Conference on Artificial Intelligence*, 2017.
- [15] M. Tan and Q. Le, "EfficientNet: Rethinking Model Scaling for Convolutional Neural Networks," in *Proceedings of the 36th International Conference on Machine Learning*. PMLR, May 2019, pp. 6105–6114.
- [16] C.-Y. Wang, I.-H. Yeh, and H.-Y. M. Liao, "YOLOv9: Learning What You Want to Learn Using Programmable Gradient Information," Feb. 2024.
- [17] M. Tan, R. Pang, and Q. V. Le, "Efficientdet: Scalable and efficient object detection," in *Proceedings of the IEEE/CVF Conference on Computer Vision and Pattern Recognition (CVPR)*, June 2020.
- [18] S. Ren, K. He, R. Girshick, and J. Sun, "Faster R-CNN: Towards Real-Time Object Detection with Region Proposal Networks," *IEEE Transactions on Pattern Analysis and Machine Intelligence*, vol. 39, no. 6, pp. 1137–1149, Jun. 2017.
- [19] K. He, G. Gkioxari, P. Dollar, and R. Girshick, "Mask R-CNN," in *2017 IEEE International Conference on Computer Vision (ICCV)*. IEEE, Oct. 2017, pp. 2980–2988.
- [20] O. Ronneberger, P. Fischer, and T. Brox, "U-net: Convolutional networks for biomedical image segmentation," in *Medical Image Computing and Computer-Assisted Intervention – MICCAI 2015*, N. Navab, J. Hornegger, W. M. Wells, and A. F. Frangi, Eds. Cham: Springer International Publishing, 2015, pp. 234–241.
- [21] N. Ravi, V. Gabeur, Y.-T. Hu, R. Hu, C. Ryali, T. Ma, H. Khedr, R. Rädle, C. Rolland, L. Gustafson, E. Mintun, J. Pan, K. V. Alwala, N. Carion, C.-Y. Wu, R. Girshick, P. Dollár, and C. Feichtenhofer, "SAM 2: Segment Anything in Images and Videos," Oct. 2024.
- [22] B. Recht, R. Roelofs, L. Schmidt, and V. Shankar, "Do ImageNet classifiers generalize to ImageNet?" in *International Conference on Machine Learning*, 2019.

- [23] F. Croce, M. Andriushchenko, V. Sehwal, E. DeBenedetti, N. Flammarion, M. Chiang, P. Mittal, and M. Hein, "Robustbench: a standardized adversarial robustness benchmark," in *Thirty-fifth Conference on Neural Information Processing Systems Datasets and Benchmarks Track (Round 2)*, 2021. [Online]. Available: <https://openreview.net/forum?id=SSKZPJct7B>
- [24] D. Hendrycks, N. Carlini, J. Schulman, and J. Steinhardt, "Unsolved problems in ML safety," *ArXiv*, vol. abs/2109.13916, 2021.
- [25] D. Hendrycks and T. Dietterich, "Benchmarking Neural Network Robustness to Common Corruptions and Perturbations," in *International Conference on Learning Representations*, 2018.
- [26] E. Mintun, A. Kirillov, and S. Xie, "On interaction between augmentations and corruptions in natural corruption robustness," in *Advances in Neural Information Processing Systems*, M. Ranzato, A. Beygelzimer, Y. Dauphin, P. Liang, and J. W. Vaughan, Eds., vol. 34. Curran Associates, Inc., 2021, pp. 3571–3583. [Online]. Available: https://proceedings.neurips.cc/paper_files/paper/2021/file/1d49780520898fe37f0cd6b41c5311bf-Paper.pdf
- [27] J. H. Metzen, T. Genewein, V. Fischer, and B. Bischoff, "On detecting adversarial perturbations," in *International Conference on Learning Representations*, 2017. [Online]. Available: <https://openreview.net/forum?id=SJzCSf9xg>
- [28] M. S. Elsayed, N.-A. Le-Khac, S. Dev, and A. D. Jurcut, "Network anomaly detection using LSTM based autoencoder," *Proceedings of the 16th ACM Symposium on QoS and Security for Wireless and Mobile Networks*, 2020.
- [29] C. Gong, D. Wang, M. Li, V. Chandra, and Q. Liu, "KeepAugment: A simple information-preserving data augmentation approach," *2021 IEEE/CVF Conference on Computer Vision and Pattern Recognition (CVPR)*, pp. 1055–1064, 2020.
- [30] D. A. Calian, F. Stimberg, O. Wiles, S.-A. Rebuffi, A. György, T. A. Mann, and S. Gowal, "Defending against image corruptions through adversarial augmentations," in *International Conference on Learning Representations*, 2022. [Online]. Available: <https://openreview.net/forum?id=jOjjiZHy3h>
- [31] J.-H. Kim, W. Choo, and H. O. Song, "Puzzle mix: Exploiting saliency and local statistics for optimal mixup," in *Proceedings of the 37th International Conference on Machine Learning*, ser. Proceedings of Machine Learning Research, H. D. III and A. Singh, Eds., vol. 119. PMLR, 13–18 Jul 2020, pp. 5275–5285.
- [32] A. Subbaswamy, R. J. Adams, and S. Saria, "Evaluating model robustness and stability to dataset shift," in *International Conference on Artificial Intelligence and Statistics*, 2021.
- [33] Z. Wang, P. Wang, K. Liu, P. Wang, Y. Fu, C.-T. Lu, C. C. Aggarwal, J. Pei, and Y. Zhou, "A Comprehensive Survey on Data Augmentation," May 2024.
- [34] A. Mumuni and F. Mumuni, "Data augmentation: A comprehensive survey of modern approaches," *Array*, vol. 16, p. 100258, 2022. [Online]. Available: <https://www.sciencedirect.com/science/article/pii/S2590005622000911>
- [35] S. Lim, I. Kim, T. Kim, C. Kim, and S. Kim, "Fast AutoAugment," in *Neural Information Processing Systems*, 2019.
- [36] E. D. Cubuk, B. Zoph, M. Mané, V. Vasudevan, and Q. V. Le, "AutoAugment: Learning augmentation strategies from data," *2019 IEEE/CVF Conference on Computer Vision and Pattern Recognition (CVPR)*, pp. 113–123, 2019.
- [37] H. Zhang, M. Cisse, Y. N. Dauphin, and D. Lopez-Paz, "mixup: Beyond empirical risk minimization," in *International Conference on Learning Representations*, 2018. [Online]. Available: <https://openreview.net/forum?id=r1Ddp1-Rb>
- [38] R. Takahashi, T. Matsubara, and K. Uehara, "RICAP: Random image cropping and patching data augmentation for deep cnns," in *Asian Conference on Machine Learning*, 2018.
- [39] J. Kim, W. Choo, H. Jeong, and H. O. Song, "Co-mixup: Saliency guided joint mixup with supermodular diversity," in *International Conference on Learning Representations*, 2021. [Online]. Available: <https://openreview.net/forum?id=gvxjzw8kW4b>
- [40] D. Hendrycks, A. Zou, M. Mazeika, L. Tang, B. Li, D. Song, and J. Steinhardt, "PixMix: Dreamlike Pictures Comprehensively Improve Safety Measures," in *Proceedings of the IEEE/CVF Conference on Computer Vision and Pattern Recognition*, 2022, pp. 16783–16792.
- [41] Z. Huang, X. Bao, N. Zhang, Q. Zhang, X. Tu, B. Wu, and X. Yang, "IPMix: Label-preserving data augmentation method for training robust classifiers," in *Proceedings of the 37th International Conference on Neural Information Processing Systems*, ser. NIPS '23. Red Hook, NY, USA: Curran Associates Inc., May 2024, pp. 63660–63673.
- [42] K. Islam, M. Z. Zaheer, A. Mahmood, and K. Nandakumar, "DiffuseMix: Label-Preserving Data Augmentation with Diffusion Models," in *Proceedings of the IEEE/CVF Conference on Computer Vision and Pattern Recognition*, 2024, pp. 27621–27630.
- [43] K. Islam, M. Z. Zaheer, A. Mahmood, K. Nandakumar, and N. Akhtar, "GenMix: Effective Data Augmentation with Generative Diffusion Model Image Editing," Dec. 2024.
- [44] S. Lloyd, "Measures of complexity: A nonexhaustive list," *IEEE Control Systems Magazine*, vol. 21, no. 4, pp. 7–8, Aug. 2001.
- [45] H. Kataoka, K. Okayasu, A. Matsumoto, E. Yamagata, R. Yamada, N. Inoue, A. Nakamura, and Y. Satoh, "Pre-training without natural images," in *Proceedings of the Asian Conference on Computer Vision (ACCV)*, November 2020.
- [46] K. Nakashima, H. Kataoka, A. Matsumoto, K. Iwata, N. Inoue, and Y. Satoh, "Can Vision Transformers Learn without Natural Images?" *Proceedings of the AAAI Conference on Artificial Intelligence*, vol. 36, no. 2, pp. 1990–1998, Jun. 2022.
- [47] H. Guo, Y. Mao, and R. Zhang, "MixUp as Locally Linear Out-of-Manifold Regularization," *Proceedings of the AAAI Conference on Artificial Intelligence*, vol. 33, no. 01, pp. 3714–3722, Jul. 2019.
- [48] R. Baena, L. Drumetz, and V. Gripon, "Local Mixup: Interpolation of closest input signals to prevent manifold intrusion," *Signal Processing*, vol. 219, p. 109395, Jun. 2024.
- [49] D. Hendrycks, K. Zhao, S. Basart, J. Steinhardt, and D. X. Song, "Natural adversarial examples," *2021 IEEE/CVF Conference on Computer Vision and Pattern Recognition (CVPR)*, pp. 15257–15266, 2019.
- [50] D. Hendrycks, S. Basart, N. Mu, S. Kadavath, F. Wang, E. Durando, R. Desai, T. L. Zhu, S. Parajuli, M. Guo, D. X. Song, J. Steinhardt, and J. Gilmer, "The many faces of robustness: A critical analysis of out-of-distribution generalization," *2021 IEEE/CVF International Conference on Computer Vision (ICCV)*, pp. 8320–8329, 2020.
- [51] Y. LeCun, L. Bottou, Y. Bengio, and P. Haffner, "Gradient-based learning applied to document recognition," *Proceedings of the IEEE*, vol. 86, no. 11, pp. 2278–2324, 1998.
- [52] A. Krizhevsky, I. Sutskever, and G. E. Hinton, "Imagenet classification with deep convolutional neural networks," in *Advances in Neural Information Processing Systems*, 2012, pp. 1097–1105.
- [53] A. Vaswani, N. Shazeer, N. Parmar, J. Uszkoreit, L. Jones, A. N. Gomez, L. u. Kaiser, and I. Polosukhin, "Attention is all you need," in *Advances in Neural Information Processing Systems*, I. Guyon, U. V. Luxburg, S. Bengio, H. Wallach, R. Fergus, S. Vishwanathan, and R. Garnett, Eds., vol. 30. Curran Associates, Inc., 2017. [Online]. Available: https://proceedings.neurips.cc/paper_files/paper/2017/file/3f5ee243547dee91fbd053c1c4a845aa-Paper.pdf
- [54] A. Dosovitskiy, L. Beyer, A. Kolesnikov, D. Weissenborn, X. Zhai, T. Unterthiner, M. Dehghani, M. Minderer, G. Heigold, S. Gelly, J. Uszkoreit, and N. Houlsby, "An Image is Worth 16x16 Words: Transformers for Image Recognition at Scale," Jun. 2021.
- [55] Z. Liu, Y. Lin, Y. Cao, H. Hu, Y. Wei, Z. Zhang, S. Lin, and B. Guo, "Swin transformer: Hierarchical vision transformer using shifted windows," in *Proceedings of the IEEE/CVF International Conference on Computer Vision*, 2021, pp. 10012–10022.
- [56] J. Ho, A. Jain, and P. Abbeel, "Denosing diffusion probabilistic models," *Advances in neural information processing systems*, vol. 33, pp. 6840–6851, 2020.
- [57] J. Sohl-Dickstein, E. Weiss, N. Maheswaranathan, and S. Ganguli, "Deep unsupervised learning using nonequilibrium thermodynamics," in *International Conference on Machine Learning*. PMLR, 2015, pp. 2256–2265.

- [58] P. Nakkiran, G. Kaplun, Y. Bansal, T. Yang, B. Barak, and I. Sutskever, "Deep double descent: Where bigger models and more data hurt," *Journal of Statistical Mechanics: Theory and Experiment*, vol. 2021, no. 12, p. 124003, 2021.
- [59] R. Gontijo-Lopes, S. J. Smullin, E. D. Cubuk, and E. Dyer, "Affinity and diversity: Quantifying mechanisms of data augmentation," *arXiv preprint arXiv:2002.08973*, 2020.
- [60] S. Yang, S. Guo, J. Zhao, and F. Shen, "Investigating the effectiveness of data augmentation from similarity and diversity: An empirical study," *Pattern Recognition*, vol. 148, p. 110204, 2024.
- [61] V. Verma, A. Lamb, C. Beckham, A. Najafi, I. Mitliagkas, D. Lopez-Paz, and Y. Bengio, "Manifold mixup: Better representations by interpolating hidden states," in *International Conference on Machine Learning*, 2018.
- [62] O. Chapelle, J. Weston, L. Bottou, and V. Vapnik, "Vicinal risk minimization," *Advances in neural information processing systems*, vol. 13, 2000.
- [63] D. Hendrycks*, N. Mu*, E. D. Cubuk, B. Zoph, J. Gilmer, and B. Lakshminarayanan, "AugMix: A Simple Data Processing Method to Improve Robustness and Uncertainty," in *International Conference on Learning Representations*, Sep. 2019.
- [64] S. G. Finlayson, J. D. Bowers, J. Ito, J. L. Zittrain, A. L. Beam, and I. S. Kohane, "Adversarial attacks on medical machine learning," *Science*, vol. 363, no. 6433, pp. 1287–1289, 2019. [Online]. Available: <https://www.science.org/doi/abs/10.1126/science.aaw4399>
- [65] N. Papernot, P. Mcdaniel, A. Sinha, and M. P. Wellman, "SoK: Security and privacy in machine learning," *2018 IEEE European Symposium on Security and Privacy (EuroS&P)*, pp. 399–414, 2018.
- [66] L. Skaf, E. Buonocore, S. Dumontet, R. Capone, and P. P. Franzese, "Applying network analysis to explore the global scientific literature on food security," *Ecol. Informatics*, vol. 56, p. 101062, 2020.
- [67] J.-J. Hwang, R. Xu, H. Lin, W.-C. Hung, J. Ji, K. Choi, D. Huang, T. He, P. Covington, B. Sapp, Y. Zhou, J. Guo, D. Anguelov, and M. Tan, "EMMA: End-to-End Multimodal Model for Autonomous Driving," Nov. 2024.
- [68] Z. Peng, W. Luo, Y. Lu, T. Shen, C. Gulino, A. Seff, and J. Fu, "Improving Agent Behaviors with RL Fine-Tuning for Autonomous Driving," in *Computer Vision – ECCV 2024*, A. Leonardis, E. Ricci, S. Roth, O. Russakovsky, T. Sattler, and G. Varol, Eds. Cham: Springer Nature Switzerland, 2025, vol. 15083, pp. 165–181.
- [69] S. Huang, L. Dong, W. Wang, Y. Hao, S. Singhal, S. Ma, T. Lv, L. Cui, O. K. Mohammed, B. Patra, Q. Liu, K. Aggarwal, Z. Chi, N. Bjorck, V. Chaudhary, S. Som, X. SONG, and F. Wei, "Language is not all you need: Aligning perception with language models," in *Advances in Neural Information Processing Systems*, A. Oh, T. Naumann, A. Globerson, K. Saenko, M. Hardt, and S. Levine, Eds., vol. 36. Curran Associates, Inc., 2023, pp. 72096–72109. [Online]. Available: https://proceedings.neurips.cc/paper_files/paper/2023/file/e425b75bac5742a008d643826428787c-Paper-Conference.pdf
- [70] Y. Shen, K. Song, X. Tan, D. Li, W. Lu, and Y. Zhuang, "Hugginggpt: Solving ai tasks with chatgpt and its friends in hugging face," in *Advances in Neural Information Processing Systems*, A. Oh, T. Naumann, A. Globerson, K. Saenko, M. Hardt, and S. Levine, Eds., vol. 36. Curran Associates, Inc., 2023, pp. 38154–38180. [Online]. Available: https://proceedings.neurips.cc/paper_files/paper/2023/file/77c33e6a367922d003ff102ffb92b658-Paper-Conference.pdf
- [71] OpenAI, J. Achiam, S. Adler *et al.*, "Gpt-4 technical report," 2024. [Online]. Available: <https://arxiv.org/abs/2303.08774>
- [72] H. Touvron, T. Lavril, G. Izacard, X. Martinet, M.-A. Lachaux, T. Lacroix, B. Rozière, N. Goyal, E. Hambro, F. Azhar, A. Rodriguez, A. Joulin, E. Grave, and G. Lample, "LLaMA: Open and Efficient Foundation Language Models," Feb. 2023.
- [73] J. Deng, W. Dong, R. Socher, L.-J. Li, K. Li, and L. Fei-Fei, "Imagenet: A large-scale hierarchical image database," in *2009 IEEE Conference on Computer Vision and Pattern Recognition*, 2009, pp. 248–255.
- [74] Y. Dong, F. Liao, T. Pang, H. Su, J. Zhu, X. Hu, and J. Li, "Boosting adversarial attacks with momentum," *2018 IEEE/CVF Conference on Computer Vision and Pattern Recognition*, pp. 9185–9193, 2017.
- [75] C. Xie, Y. Wu, L. van der Maaten, A. L. Yuille, and K. He, "Feature denoising for improving adversarial robustness," *2019 IEEE/CVF Conference on Computer Vision and Pattern Recognition (CVPR)*, pp. 501–509, 2018.
- [76] C. Xie, M. Tan, B. Gong, J. Wang, A. L. Yuille, and Q. V. Le, "Adversarial examples improve image recognition," *2020 IEEE/CVF Conference on Computer Vision and Pattern Recognition (CVPR)*, pp. 816–825, 2019.
- [77] D. Bashkirova, D. Hendrycks, D. Kim, H. Liao, S. Mishra, C. Rajagopalan, K. Saenko, K. Saito, B. U. Tayyab, P. Teterwak, and B. Usman, "Visda-2021 competition: Universal domain adaptation to improve performance on out-of-distribution data," in *Proceedings of the NeurIPS 2021 Competitions and Demonstrations Track*, ser. Proceedings of Machine Learning Research, D. Kiela, M. Ciccone, and B. Caputo, Eds., vol. 176. PMLR, 06–14 Dec 2022, pp. 66–79. [Online]. Available: <https://proceedings.mlr.press/v176/bashkirova22a.html>
- [78] L. Ruff, J. R. Kauffmann, R. A. Vandermeulen, G. Montavon, W. Samek, M. Kloft, T. G. Dietterich, and K.-R. Müller, "A unifying review of deep and shallow anomaly detection," *Proceedings of the IEEE*, vol. 109, no. 5, pp. 756–795, 2021.
- [79] D. Yin, R. Gontijo Lopes, J. Shlens, E. D. Cubuk, and J. Gilmer, "A fourier perspective on model robustness in computer vision," in *Advances in Neural Information Processing Systems*, H. Wallach, H. Larochelle, A. Beygelzimer, F. d'Alché-Buc, E. Fox, and R. Garnett, Eds., vol. 32. Curran Associates, Inc., 2019. [Online]. Available: https://proceedings.neurips.cc/paper_files/paper/2019/file/b05b57f6add810d3b7490866d74c0053-Paper.pdf
- [80] S. Sagawa*, P. W. Koh*, T. B. Hashimoto, and P. Liang, "Distributionally robust neural networks," in *International Conference on Learning Representations*, 2020. [Online]. Available: <https://openreview.net/forum?id=ryxGuJrFvS>
- [81] P. W. Koh, S. Sagawa, H. Marklund, S. M. Xie, M. Zhang, A. Balsubramani, W. Hu, M. Yasunaga, R. L. Phillips, I. Gao, T. Lee, E. David, I. Stavness, W. Guo, B. Earnshaw, I. Haque, S. M. Beery, J. Leskovec, A. Kundaje, E. Pierson, S. Levine, C. Finn, and P. Liang, "Wilds: A benchmark of in-the-wild distribution shifts," in *Proceedings of the 38th International Conference on Machine Learning*, ser. Proceedings of Machine Learning Research, M. Meila and T. Zhang, Eds., vol. 139. PMLR, 18–24 Jul 2021, pp. 5637–5664. [Online]. Available: <https://proceedings.mlr.press/v139/koh21a.html>
- [82] R. Geirhos, P. Rubisch, C. Michaelis, M. Bethge, F. A. Wichmann, and W. Brendel, "Imagenet-trained CNNs are biased towards texture; increasing shape bias improves accuracy and robustness." in *International Conference on Learning Representations*, 2019. [Online]. Available: <https://openreview.net/forum?id=Bygh9j09KX>
- [83] C. Guo, G. Pleiss, Y. Sun, and K. Q. Weinberger, "On calibration of modern neural networks," in *Proceedings of the 34th International Conference on Machine Learning*, ser. Proceedings of Machine Learning Research, D. Precup and Y. W. Teh, Eds., vol. 70. PMLR, 06–11 Aug 2017, pp. 1321–1330. [Online]. Available: <https://proceedings.mlr.press/v70/guo17a.html>
- [84] V. Kuleshov, N. Fenner, and S. Ermon, "Accurate uncertainties for deep learning using calibrated regression," in *Proceedings of the 35th International Conference on Machine Learning*, ser. Proceedings of Machine Learning Research, J. Dy and A. Krause, Eds., vol. 80. PMLR, 10–15 Jul 2018, pp. 2796–2804. [Online]. Available: <https://proceedings.mlr.press/v80/kuleshov18a.html>
- [85] Y. Ovadia, E. Fertig, J. Ren, Z. Nado, D. Sculley, S. Nowozin, J. Dillon, B. Lakshminarayanan, and J. Snoek, "Can you trust your model's uncertainty? evaluating predictive uncertainty under dataset shift," in *Advances in Neural Information Processing Systems*, H. Wallach, H. Larochelle, A. Beygelzimer, F. d'Alché-Buc, E. Fox, and R. Garnett, Eds., vol. 32. Curran Associates, Inc., 2019. [Online]. Available: https://proceedings.neurips.cc/paper_files/paper/2019/file/8558cb408c1d76621371888657d2eb1d-Paper.pdf
- [86] C. Anderson and R. Farrell, "Improving fractal pre-training," *2022 IEEE/CVF Winter Conference on Applications of Computer Vision (WACV)*, pp. 2412–2421, 2021.
- [87] A. Krizhevsky and G. Hinton, "Learning multiple layers of features from tiny images," 2009.
- [88] O. Russakovsky, J. Deng, H. Su, J. Krause, S. Satheesh, S. Ma, Z. Huang, A. Karpathy, A. Khosla, and M. Bernstein, "Imagenet large scale visual recognition challenge," *International Journal of Computer Vision*, vol. 115, no. 3, pp. 211–252, 2015.

- [89] I. J. Good, "Some terminology and notation in information theory," *Proceedings of the IEE-Part C: Monographs*, vol. 103, no. 3, pp. 200–204, 1956.
- [90] S. Yun, D. Han, S. J. Oh, S. Chun, J. Choe, and Y. J. Yoo, "CutMix: Regularization strategy to train strong classifiers with localizable features," *2019 IEEE/CVF International Conference on Computer Vision (ICCV)*, pp. 6022–6031, 2019.
- [91] A. Madry, A. Makelov, L. Schmidt, D. Tsipras, and A. Vladu, "Towards deep learning models resistant to adversarial attacks," in *International Conference on Learning Representations*, 2018. [Online]. Available: <https://openreview.net/forum?id=rJzIBfZAb>
- [92] D. Hendrycks, M. Mazeika, and T. Dietterich, "Deep anomaly detection with outlier exposure," in *International Conference on Learning Representations*, 2019.
- [93] K. Nguyen and B. O'Connor, "Posterior calibration and exploratory analysis for natural language processing models," in *EMNLP*. Lisbon, Portugal: Association for Computational Linguistics, 2015, pp. 1587–1598. [Online]. Available: <https://www.aclweb.org/anthology/D15-1182>
- [94] I. Loshchilov and F. Hutter, "SGDR: Stochastic gradient descent with warm restarts," in *International Conference on Learning Representations*, 2017. [Online]. Available: <https://openreview.net/forum?id=Skq89Scxx>
- [95] S. Xie, R. Girshick, P. Dollár, Z. Tu, and K. He, "Aggregated residual transformations for deep neural networks," in *Proceedings of the IEEE Conference on Computer Vision and Pattern Recognition (CVPR)*, July 2017.
- [96] Y. Le and X. Yang, "Tiny imagenet visual recognition challenge," *CS 231N*, vol. 7, no. 7, p. 3, 2015.
- [97] X. Zhang, Q. Wang, J. Zhang, and Z. Zhong, "Adversarial autoaugment," in *International Conference on Learning Representations*, 2020. [Online]. Available: <https://openreview.net/forum?id=ByxdUySKvS>
- [98] S. G. Müller and F. Hutter, "TrivialAugment: Tuning-free yet state-of-the-art data augmentation," *2021 IEEE/CVF International Conference on Computer Vision (ICCV)*, pp. 754–762, 2021.
- [99] P. May, "Improved image augmentation for convolutional neural networks by copyout and coppingairing," 2020. [Online]. Available: <https://openreview.net/forum?id=rkxWpCNKvS>
- [100] A. F. M. S. Uddin, M. S. Monira, W. Shin, T. Chung, and S.-H. Bae, "Saliency mix: A saliency guided data augmentation strategy for better regularization," in *International Conference on Learning Representations*, 2021. [Online]. Available: <https://openreview.net/forum?id=-M0QkvBGTtq>
- [101] Z. Liu, S. Li, D. Wu, Z. Chen, L. Wu, J. Guo, and S. Z. Li, "AutoMix: Unveiling the power of mixup for stronger classifiers," in *European Conference on Computer Vision*, 2021.
- [102] J. Liu, B. Liu, H. Zhou, H. Li, and Y. Liu, "TokenMix: Rethinking image mixing for data augmentation in vision transformers," in *European Conference on Computer Vision*, 2022.
- [103] J.-H. Lee, M. Z. Zaheer, M. Astrid, and S.-I. Lee, "SmoothMix: A Simple Yet Effective Data Augmentation to Train Robust Classifiers," in *Proceedings of the IEEE/CVF Conference on Computer Vision and Pattern Recognition Workshops*, 2020, pp. 756–757.
- [104] E. Harris, A. Marcu, M. Painter, M. Niranjana, A. Prugel-Bennett, and J. Hare, "Fmix: Enhancing mixed sample data augmentation," 2021. [Online]. Available: <https://openreview.net/forum?id=oev4KdikGjy>
- [105] C.-L. Li, K. Sohn, J. Yoon, and T. Pfister, "CutPaste: Self-supervised learning for anomaly detection and localization," *2021 IEEE/CVF Conference on Computer Vision and Pattern Recognition (CVPR)*, pp. 9659–9669, 2021.
- [106] D. B. Walther and D. Shen, "Nonaccidental properties underlie human categorization of complex natural scenes," *Psychological Science*, vol. 25, no. 4, pp. 851–860, 2014, pMID: 24474725. [Online]. Available: <https://doi.org/10.1177/0956797613512662>

APPENDIX A RELEATED WORK.

This section provides a comprehensive overview of our work’s foundational components, focusing on data augmentation, complex image mixing strategies, and robustness evaluation benchmarks.

A.1 Data Augmentation

A.1.1 Image Augmentations

These augmentations operate independently on a single data sample, introducing variations without relying on other samples from the dataset. Transformations of this type often generate samples that are closely clustered within the feature space. Examples include spatial transformations and affine manipulations [2], [35], [36]. Additionally, policy-driven augmentations have gained traction in recent years. AutoAugment [36], for instance, employs reinforcement learning to automatically discover optimal augmentation policies, while AdversarialAutoAugment [97] generates adversarial examples to dynamically adjust augmentation strategies during training.

Randomization-based approaches like RandomAugment [2] simplified the policy search by randomly applying augmentation operations in the sequence to generate unique synthetic samples. TrivialAugment [98] further extended it by applying only one augmentation operation in a pipeline. They sampled random corruption magnitude from a uniform distribution everytime, making them computationally efficient. Other notable methods include localized augmentation techniques such as CutOut [99] and RandomErase [3] which randomly masks regions of an image to compel models to rely on broader spatial features, thereby improving generalization.

A.1.2 Image Blending

Image blending techniques leverage pixel-level mixing strategies to create diverse augmented samples. These methods often involve pixel-wise weighted averages to combine information from multiple images, enhancing robustness and generalization. MixUp [37] generates augmented samples by linearly interpolating between two randomly selected images and their corresponding labels, encouraging smoother decision boundaries for classification tasks. Manifold-MixUp [61] performs similar interpolations within the hidden layers of a neural network, leading to improved accuracy by enforcing smooth transitions between feature representations.

CutMix [90] introduces a patch-based approach, replacing a region of one image with a corresponding patch from another, while blending their labels proportionally to the patch size. This method enhances performance by encouraging

the network to focus on multiple regions of interest. SaliencyMix [100] uses saliency maps to guide augmentation, replacing a square patch of the original image with the most salient regions from another image. This strategy ensures that the inserted regions carry highly informative features, thereby improving model learning.

AugMix [63] introduced a novel strategy by combining multiple transformations to produce diverse and robust augmented images, achieving state-of-the-art performance in robustness to corruptions and calibration tasks. Similarly, AutoMix [101] employs a bi-level optimization framework to simultaneously improve the generation of mixed samples and the training of classifiers, achieving significant gains in robustness and accuracy. TokenMix [102], designed for Vision Transformers, partitions images into multiple distinct regions at the token level and mixes them to exploit the unique properties of transformer architectures, resulting in better performance on vision tasks. PuzzleMix [31], SmoothMix [103], FMix [104], LocalMixup [48], CutPaste [105] are few other models having similar topology.

A.1.3 Fractal-Based Augmentations

Fractals also known as non-natural images, are images with complex structures. They have intriguing properties that humans often rely on for perception. Such properties include structural characteristics of contours—such as orientation, length, and curvature—and junction types and angles derived from natural scene line drawings [106].

Fractal-based augmentation methods introduce structural complexity to the augmentation process by incorporating mathematically intricate patterns or synthetic structures to generate the labels-preserved samples that avoid the Manifold Intrusion [47], [48] due to MixUp based approaches [37]. PixMix [40] combines natural images with fractals and feature visualizations, which serve as highly diverse and complex augmentations to boost model robustness. They observed a significant accuracy boost for the out-of-domain benchmarks. IPMix [41] adopts a three-stage approach, integrating images, patch, and pixel-based approach in label-preserving mixing strategies to generate robust training samples. Recent methods such as DiffuseMix [42] and GenMix [43] blended the samples augmented through the Diffusion model with complex fractals and noticed the accuracy improvement.

APPENDIX B GRAY-SCALE FRACTALS.

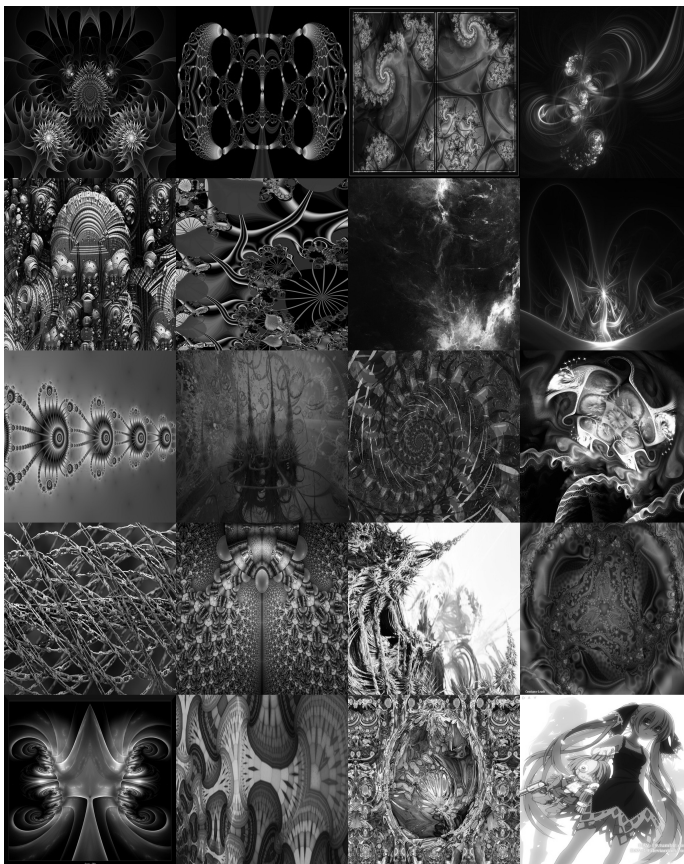


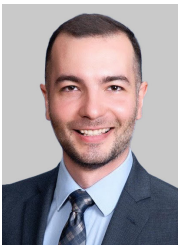
Fig. 5: Samples of grayscale fractals we used.



Hafiz Mughees Ahmad completed his Bachelor's and Master's in Electrical Engineering from the Institute of Space Technology, Pakistan, in 2015 and 2018, respectively. He is currently pursuing a Ph.D. at the University of Windsor, Canada. Alongside his studies, he serves as a Deep Learning Engineer at IFIVEO CANADA INC. His previous roles include Research Associate at Istanbul Medipol University, Turkey, and Lecturer at the Institute of Space Technology, Pakistan. His research focuses on Computer Vision and Deep Learning, with applications in Object Detection and real-time surveillance and monitoring in the production environment. He is a Graduate Student Member of IEEE.



Dario Morle completed his Bachelor's in Electrical Engineering from the University of Windsor, Canada. During his undergraduate degree, Dario assisted in research at both the Center for Computer Vision and Deep Learning, and the Human Systems Lab. After graduating in 2022, he joined IFIVEO CANADA INC. as a Deep Learning Engineer where he worked on developing and deploying computer vision solutions for industrial applications. His research interests include neural architecture design, energy-based models, and applications to industrial processes.



Afshin Rahimi received his B.Sc. degree from the K. N. Toosi University of Technology, Tehran, Iran, in 2010, and the M.Sc. and Ph.D. degrees from Toronto Metropolitan University, Toronto, ON, Canada, in 2012, and 2017, respectively, in Aerospace Engineering. He was with Pratt & Whitney Canada from 2017 to 2018. Since 2018, he has been an Associate Professor in the Department of Mechanical, Automotive, and Materials Engineering at the University of Windsor, Windsor, ON, Canada. Since 2010, he has been involved in various industrial research, technology development, and systems engineering projects/contracts related to the control and diagnostics of satellites, UAVs, and commercial aircraft subsystems. In recent years, he has also been involved with industrial automation and using technologies to boost manual labor work in industrial settings. He is a senior member of IEEE, a lifetime member of AIAA, and a technical member of the PHM Society.